Improved spatial characterization of the epileptic brain by focusing on nonlinearity

Ralph G. Andrzejak [a,b,*], Florian Mormann [b], Guido Widman [b],
Thomas Kreuz [a,b,1], Christian E. Elger [b], Klaus Lehnertz [b,c]

[a] *John von Neumann Institute for Computing, Forschungszentrum Jülich GmbH, Jülich, Germany*
[b] *Department of Epileptology, University of Bonn, Sigmund Freud Str. 25, D-53105 Bonn, Germany*
[c] *Helmholtz Institute for Radiation and Nuclear Physics, University of Bonn, Germany*

Abstract

An advanced characterization of the complicated dynamical system brain is one of science's biggest challenges. Nonlinear time series analysis allows characterizing nonlinear dynamical systems in which low-dimensional nonlinearity gives rise to complex and irregular behavior. While several studies indicate that nonlinear methods can extract valuable information from neuronal dynamics, others doubt their necessity and conjecture that the same information can be obtained using classical linear techniques. To address this issue, we compared these two concepts, but included furthermore a combination of nonlinear measures with surrogates, an approach that has been designed to specifically focus on nonlinearity. As a benchmark we used the discriminative power to detect the seizure-generating hemisphere in medically intractable mesial temporal lobe epilepsy. We analyzed intracranial electroencephalographic recordings from the seizure-free interval of 29 patients. While the performance of both linear and nonlinear measures was weak, if not insignificant, a very high performance was obtained by the use of surrogate-corrected measures. Focusing on nonlinearity by using a combination of nonlinear measures with surrogates appears as the key to a successful characterization of the spatial distribution of the epileptic process.

1. Introduction

In recent years a localization of epileptic foci from the electroencephalogram (EEG) recorded during the seizure-free interval has been attempted using different time series analysis techniques. Time series analysis comprises different concepts for an optimal

---
* Corresponding author at: Universitat Pompeu Fabra, Passeig de Circumval·lació, 8, 08003 Barcelona, Spain. Tel.: +34 93 542 2936; fax: +34 93 542 2451.

    E-mail address: ralphandrzejak@yahoo.de (R.G. Andrzejak).
[1] Istituto dei Sistemi Complessi, CNR, Florence, Italy.

characterization of different classes of dynamical systems. Measures derived from linear time series analysis (LTSA (Box and Jenkins, 1976)) are most appropriate for the description of systems in which cause and effect are proportional. Well-known LTSA measures are the delta-, alpha-, theta-, beta-, and gamma-band power that are extracted from the power spectrum and quantify the amount of activity in specified frequency ranges. LTSA measures, however, are not sensitive to certain properties specific to nonlinear deterministic dynamical systems. A characterization of nonlinear deterministic dynamics, in which stimulus and response are related by other than linear relations, can be achieved by means of nonlinear time series analysis (NTSA), the practical spin-off from the theory of deterministic chaos (Kantz and Schreiber, 1997). Prominent NTSA measures are the Lyapunov exponent and the correlation dimension, designed to identify chaotic behavior in deterministic dynamics and to estimate their dimensionality. In early studies, evidence for deterministic chaos in various neuronal dynamics was derived from applications of these measures to the EEG (Babloyantz and Destexhe, 1986; Frank et al., 1990). However, it was soon demonstrated that NTSA measures are sensitive to properties of nonlinear deterministic dynamics without being very specific (e.g. Osborne and Provenzale, 1989), and the interpretation of NTSA results obtained for some unknown dynamics can be quite problematic (Kantz and Schreiber, 1997). These problems led to the development of the concept of surrogate time series (Schreiber and Schmitz, 1996, 2000), some roots of which can be found in the context of the analysis of the EEG (Pijn et al., 1991). Formally, surrogate time series allow testing whether results obtained from NTSA measures are consistent with the null hypothesis that the time series was measured from a linear stochastic dynamics. A combination of NTSA measures with the concept of surrogates, which we will refer to as surrogate time series analysis (STSA), can be expected to isolate the specific nonlinear features of the time series.

A number of studies investigated whether a localization of the focal area can be obtained from seizure-free EEG recordings, using measures derived from LTSA (Nuwer, 1988; Panet-Raymond and Gotman, 1990; Marciani et al., 1992; Wang and Wieser, 1994; Tuunainen et al., 1995; Gambardella et al., 1995; Drake et al., 1998), NTSA (Lehnertz and Elger, 1995; Pijn et al., 1997; Weber et al., 1998; Mormann et al., 2000; Widman et al., 2000), or STSA (Casdagli et al., 1997; Andrzejak et al., 2001a). Most of these studies achieved promising results by rendering a correct localization in a high percentage of cases. A comparison of the performance of these different approaches, however, is still missing and cannot be derived from these studies as they were carried out on different collectives of patients and different types of epilepsy. Comparability is furthermore diminished by the fact that some studies were based on the analysis of surface EEG recordings while others analyzed intracranial EEG. The aim of the present study was therefore to carry out a comparison of the different approaches, i.e. LTSA, NTSA, and STSA, with regard to the discriminative power of the different techniques for the detection of the focal hemisphere in epilepsy patients from intracranial EEG recordings during the seizure-free interval.

2. Methods

2.1. Patients and EEG recordings

The analyzed EEG signals were recorded from 29 epilepsy patients with medically intractable focal epilepsies undergoing invasive presurgical diagnostics between 1993 and 2000 at the Department of Epileptology of the University of Bonn, Germany, by means of intracranially implanted electrodes. We chose these data sets since they were recorded from patients with "classical" unilateral mesial temporal lobe epilepsy (MTLE) including signs of hippocampal sclerosis in the MRI and ipsilateral seizure onset in the scalp EEG. Invasive presurgical evaluation yielded electrographical seizure onset in the depth electrode of the sclerotic hippocampus in all cases. According to the current state of the art in epileptology invasive EEG recordings are no longer necessary in these classical cases of unilateral MTLE since noninvasive diagnostics is considered sufficient. The data sets were thus selected for their homogeneity as opposed to the more complicated types of epilepsy that still require invasive diagnostics nowadays.

Selective amygdalohippocampectomy (18 left, 11 right) led to post-operative complete seizure control in all cases documented for at least 1 year (mean: 3.8 years, range: 1–9 years). We retrospectively analyzed

a total of 84 EEG recordings with an average length of 130 min per patient (range: 19–585 min). All recordings were performed prior to and independently from the design of this study. During the recordings, patients were awake and at rest. Recorded epochs as selected by EEG technicians at the time of acquisition included both the normal baseline EEG prior to medical tapering as well as typical interictal activity for an individual patient. Any data recorded during the pre-ictal period (1 h before seizure) or post-ictal period (2 h after seizure) as well as periods containing artifacts were discarded. No other selection was carried out.

The EEG was recorded via intrahippocampal depth electrodes (Fig. 1), each equipped with 10 cylindrical contacts (length: 2.5 mm, intercontact distance: 4 mm). These electrodes were implanted stereotactically via the longitudinal axis of the hippocampus using an occipital approach with the amygdala as target for the most anterior electrode contact (cf. Van Roost et al., 1998). After neurosurgical implantation, the correct placement of the electrodes was verified by magnetic resonance imaging. EEG recordings were performed at a sampling frequency of 173.61 Hz using a 12 bit analog to digital (A/D) converter and was band-pass
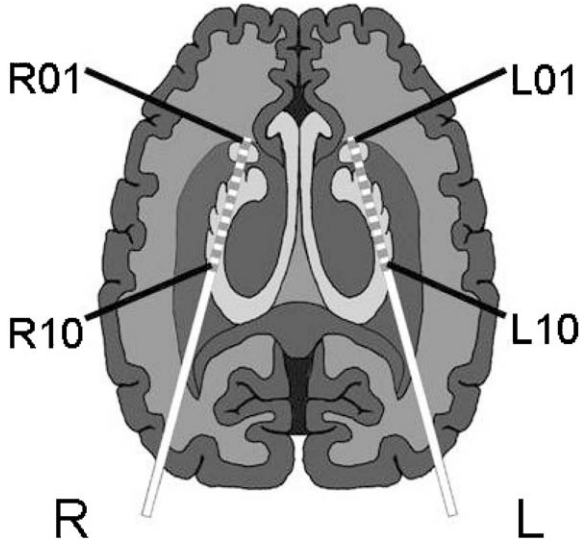

Fig. 1. Scheme of bilateral intra-hippocampal depth electrodes, each equipped with 10 cylindrical contacts. Electrodes were implanted stereotactically via the longitudinal axis of the hippocampal formation using an occipital approach. After implantation, correct electrode placement was verified using magnetic resonance imaging.

filtered from 0.5 to 85 Hz (12 dB/oct.). Apart from the approval by the local medical ethics committee, informed consent for the study was obtained from all patients.

2.2. Time series analysis

For each of the analysis concepts (LTSA, NTSA, STSA) we chose four representative measures. As LTSA measures we used the relative power in the delta-band (DP (Niedermeyer and Lopes da Silva, 1999)), i.e., the fraction of power contained in the frequency range of 0.5–4 Hz, the decay time of the autocorrelation function (DT (Box and Jenkins, 1976)), the skewness of the amplitude distribution (SK (Box and Jenkins, 1976)), and the second statistical moment of the power spectrum often referred to as Hjorth mobility (HM (Hjorth, 1970)).

As NTSA measures we used the nonlinear prediction error PE (Kantz and Schreiber, 1997; Andrzejak et al., 2001b) and the local flow LF (Kantz and Schreiber, 1997; Andrzejak et al., 2001a). Based on different approaches both of these statistics are designed as tests for nonlinear determinism. Furthermore, we used an effective correlation dimension CD (Grassberger and Procaccia, 1983; Lehnertz and Elger, 1995) as an estimate of the number of active degrees of freedom, and the algorithmic complexity AC (Lempel and Ziv, 1976; Kasper and Schuster, 1987) which is derived from the theory of symbolic dynamics and can be regarded as an estimate of the entropy of the dynamics. All NTSA measures used in this study require selection of a set of parameters. In order to avoid any in-sample optimization, which would lead to an over-estimation of the discriminative power of the NTSA measures, we used the same parameters as in previous studies of our group CD (Lehnertz and Elger, 1995), LF (Andrzejak et al., 2001a), PE (Andrzejak et al., 2001b), and AC (Mormann et al., 2005), for which these parameters were determined from pre-analyses carried out on model dynamics and on exemplary EEG segments. All parameters along with detailed descriptions of all measures are provided in the Appendix A.

For each NTSA measure a corresponding STSA measure was calculated as follows. For each EEG time series a set of nine surrogate time series was generated, and the NTSA measure was calculated for both the original EEG and its surrogates. The STSA measure

was calculated as the NTSA measure obtained for the original time series minus the mean value obtained for the set of surrogates (Schreiber and Schmitz, 2000). As noted above, the surrogates' distribution represents the results that would be expected for a linear stochastic process having the same power spectrum and amplitude distribution as the original time series. Therefore, subtracting the mean value of the surrogates' distribution from the result obtained for the original can be regarded as an offset correction, where the offset is given by the linear properties of the dynamics. For the formal definition of the STSA measures and details on the algorithm used to generate surrogate time series, refer to the Appendix A.

All recordings were analyzed using a moving window technique, with a segment length of 4096 samples and 50% overlap of consecutive segments. The starting point of each segment was slightly shifted in such a way that the two ends of each window matched in amplitude and in slope (Ehlers et al., 1998; Andrzejak et al., 2001a,b). This was necessary since for the calculation of the discrete Fourier transform a time series is implicitly assumed as one period of a continuous signal, and hence, discontinuities between the two ends of an otherwise smooth signal would cause spurious frequency components. This artifact would affect measures derived from the power spectrum and a proper generation of the surrogates. The required shifts were typically in the order of 1–2% of the segment length. Provided that such small shifts are irrelevant for subsequent steps of analysis, as it was the case for the present study, their use can replace windowing techniques that are otherwise used to address the problem of end-to-end discontinuities.

3. Results

Exemplary profiles of three representative measures (DP, LF and S-LF) calculated from one EEG recording demonstrate a substantial variability over time and different contacts. These examples also illustrate the degree to which values of LTSA, NTSA, and STSA measures are correlated to each other (Fig. 2). For a further evaluation we carried out two steps of averaging: for every patient, values were averaged over time comprising all recordings analyzed for this patient. Subsequently these values were averaged over the 10 contacts

of each of the two electrodes. As illustrated for DP, LF and S-LF, the resulting mean values exhibit a high inter-patient variability as well as asymmetries with regard to the focal and non-focal hemisphere (Figs. 2 and 3). To evaluate the significance of these asymmetries we applied an analysis of variance (ANOVA) using F-statistics to the differences between mean values of the left and right hemisphere along with the corresponding sides of the focal hemisphere. If the analysis of variance resulted in a significant F-value, a discriminant analysis was carried out (Fig. 3 and Table 1).

For the group of LTSA measures up to 83% of the cases investigated here were correctly classified. In contrast, the discriminative power of NTSA measures for the focal hemisphere was rather poor (up to 72% for CD) if not insignificant. A completely different picture, however, was established when surrogates were used in combination with NTSA measures: the performance of STSA measures was always higher than the performance of the corresponding NTSA measures and reached values of up to 93%. And even the weakest performer of the STSA group (S-PE with 86%) still surpassed the overall best performer of the other two groups (DP with 83%).

In earlier studies a correct lateralization of the focal hemisphere was obtained in 20 out of 20 patients with temporal lobe epilepsy using the measure CD (Lehnertz and Elger, 1995), and in 25 out of 25 patients with mesial temporal lobe epilepsy using the 'fraction of nonlinear determinism' (Andrzejak et al., 2001a), a measure closely related to S-LF. The performance obtained in the present study for CD and S-LF is weaker. We attribute this discrepancy to the fact that smaller groups of patients and in particular smaller samples of EEG recordings per patient were investigated in Refs. (Lehnertz and Elger, 1995; Andrzejak et al., 2001a), which may not represent an adequate sample of MTLE patients.

Finally, we shall consider exemplary EEG time series to illustrate the influence of interictal epileptiform activity and nonstationarity on STSA values (Figs. 4 and 5). For EEG time series nonstationary features are often caused by epileptiform activity: time series, which contain single isolated interictal epileptiform events, exhibit a nonstationary appearance (cf. examples 7–10 in Figs. 4 and 5). If, on the other hand, these interictal epileptiform events are recurrent and frequent in a given time series they can be regarded as
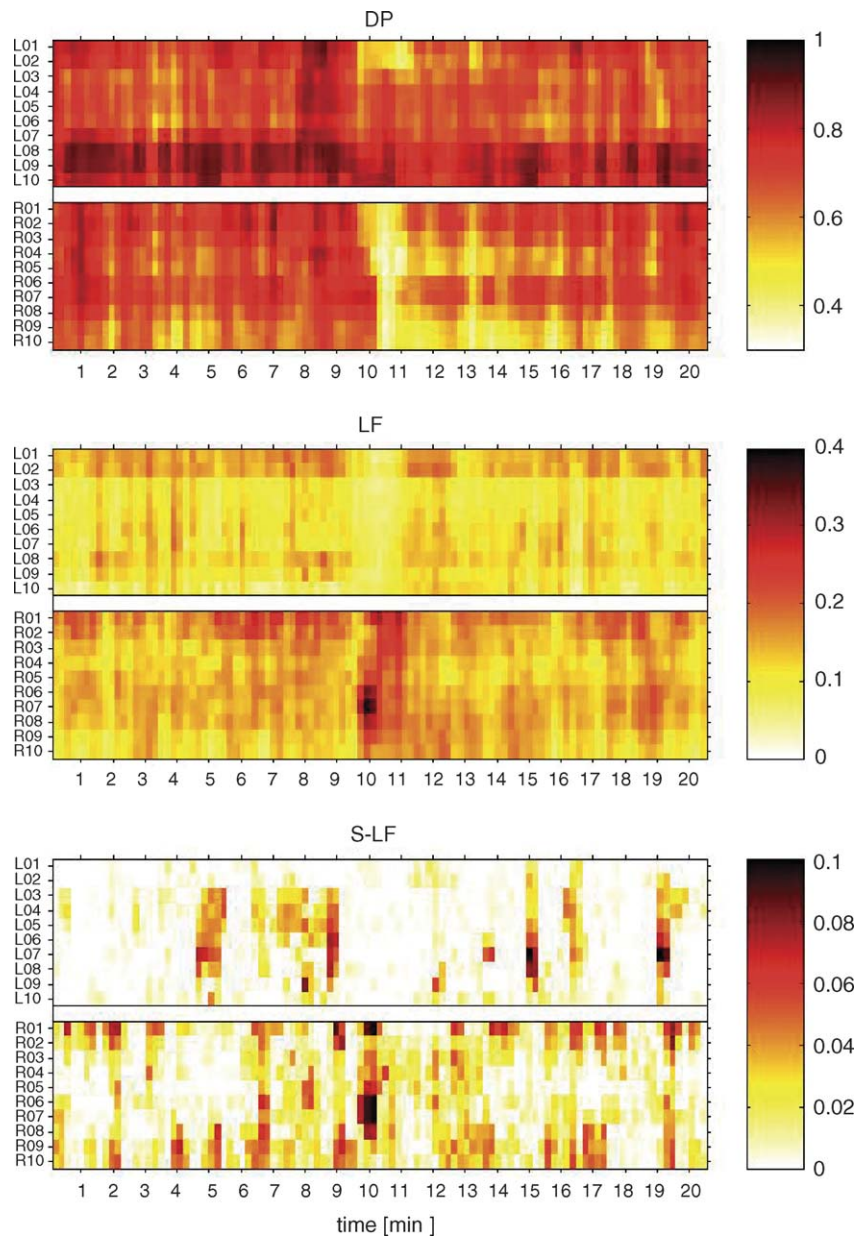
Fig. 2. Color-scaled values of DP, LF, and S-LF for an exemplary EEG recording from a patient with right mesial temporal lobe epilepsy. Rows denoted with L01-L10 and R01-R10 correspond to results obtained for the EEG recorded in the left and right hemisphere, respectively (cf. Fig. 1). These profiles demonstrate the degree to which values of LTSA, NTSA, and STSA measures correlate: for both LF and S-LF, on average higher values were calculated for contacts R01-R10 than for contacts L01-L10. Note in particular the local maximum for R06-R08 in values of both measures around minute 10. A closer look, however, reveals also a number of outstanding differences: for instance, distinct high S-LF values found for contacts L03-L10 for minutes 5, 9, 15, and 19 form patterns that cannot be found in the profile of LF values. Furthermore, higher LF values for L01-L02, L08-L09, R01, and R05-R07 did not result in high values of S-LF for these contacts, but a comparable signature can be found in the profile of DP values. Finally, rather few correlations can be found between the profiles of S-LF and DP.
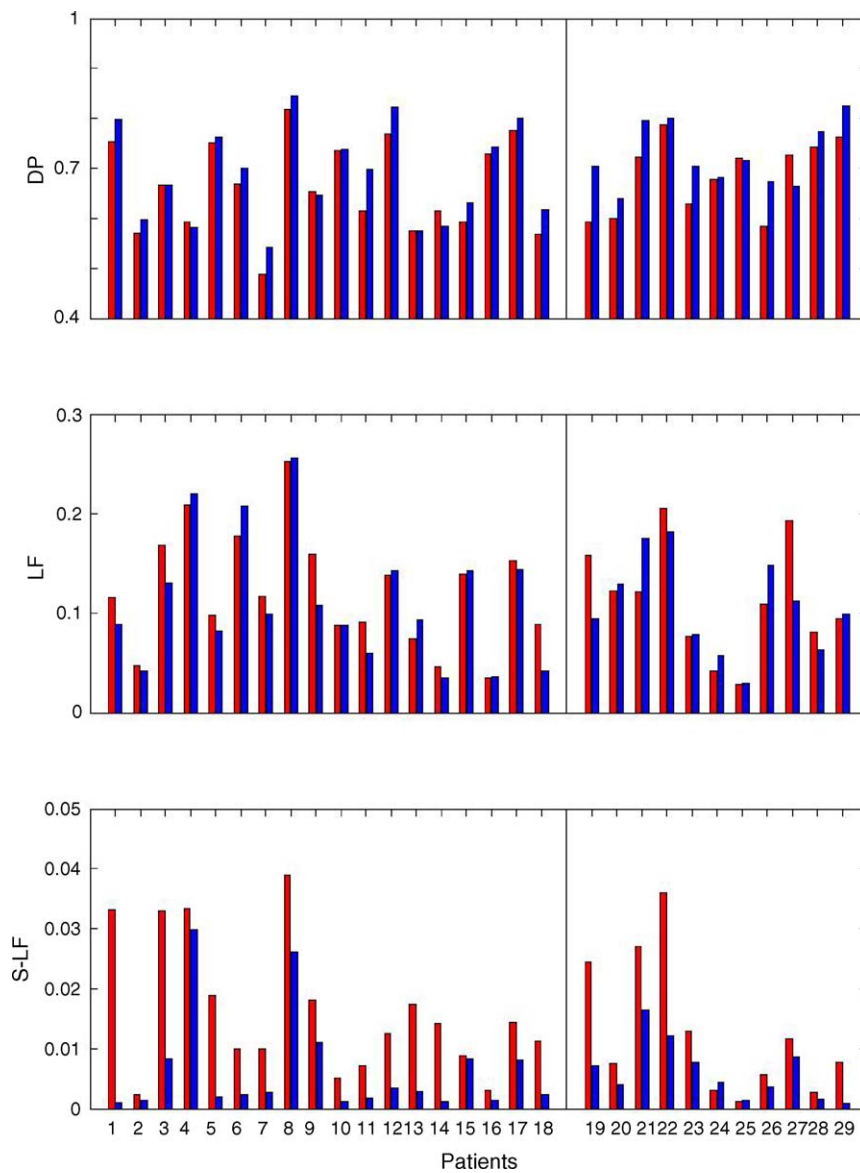
Fig. 3. Results of DP, LF and S-LF for all patients: mean values over time and over the 10 contacts of the electrodes of the focal and non-focal hemisphere depicted by red and blue bars, respectively. Note in that all but five cases higher values of DP are obtained for the focal hemisphere. While no such clear tendency is established for LF in all but two cases higher values of S-LF are obtained for the focal hemisphere.

intermittent but typical events of a stationary dynamics. Accordingly, the time series can have an overall stationary appearance (cf. examples 5–6).

Formally, the type of surrogates used for the calculation of the STSA measures allows testing of the null hypothesis that the time series was measured from a stationary Gaussian linear stochastic dynamics by means of a static and invertible measurement function. Since stationarity is explicitly included in this null hypotheses it is often argued that high values of STSA measures might simply reflect strong nonstationarity of the dynamics. The given examples illustrate, however, that nonstationarity is neither necessary nor sufficient to cause high values of STSA measures (see Fig. 5).

Table 1
An analysis of variance was used to test for a significant influence of the side of the focal hemisphere on the inter-hemispheric differences of the particular measure

Measure		*F*	#	%	Diff.
LTSA					
Delta power	DP	18.6	24	83	Lower
Decay time	DT	24.4	23	79	Lower
Skewness	SK	8.2	21	72	Higher
Hjorth mobility	HM	0.9	–	–	–
NTSA					
Local flow	LF	1.9	–	–	–
Prediction error	PE	5.1	18	62	Lower
Correlation dimension	CD	13.3	21	72	Lower
Algorithmic complexity	AC	1.4	–	–	–
STSA					
Surrogate-corrected local flow	S-LF	27.5	27	93	Higher
Surrogate-corrected prediction error	S-PE	12.4	25	86	Higher
Surrogate-corrected correlation dimension	S-CD	19.1	26	90	Higher
Surrogate-corrected algorithmic complexity	S-AC	13.6	26	90	Higher

A discriminant analysis was carried out for *F*-values higher than 2.7 (cf. second column). The resulting number and percentage of correct classifications is given in the third and fourth column, respectively. Dashes are used for measures for which non-significant *F*-values were obtained. Entries in the fifth column indicate whether higher or lower values of the respective measure were obtained for the focal hemisphere in comparison with the non-focal hemisphere (cf. Appendix A).

While high STSA values can indeed be obtained for clearly nonstationary time series (examples 9–10), they can also be obtained for comparably stationary time series (examples 3–6). Furthermore, zero STSA values can be obtained for nonstationary time series (examples 7–8). A detailed discussion of this phenomenon is given in the Appendix A. We report furthermore, that recurrent epileptiform activity, which does not distort the stationarity of the EEG (examples 5–6), is typically sufficient to cause high values of STSA measures, but EEG time series which do not exhibit prominent epileptiform events can also result in high STSA values (examples 3–4).

4. Discussion

Our results demonstrate a substantial advantage of STSA over NTSA and LTSA techniques for the lateralization or even localization of the epileptic focus from interictal EEG recordings. In two aspects we do believe in the generality of this conclusion. First we are confident that analogous findings should be obtained for other representatives of the three analysis concepts. Furthermore, we expect that our findings can

be extrapolated to other types of epilepsy besides focal mesial temporal lobe epilepsy and perhaps also to non-invasive EEG recordings. In particular, cases of lesional neocortical epilepsy could be studied to test whether STSA measures are superior for a precise localization of the focal area. Doubtlessly, different answers might be obtained in the context of other problems such as the prediction of epileptic seizures (Paluš et al., 1999; Kugiumtzis and Larson, 2000; Mormann et al., 2003; Andrzejak et al., 2003a; McSharry et al., 2003; Li et al., 2003; Winterhalder et al., 2003; Mormann et al., 2005; and references therein) or the investigation of other pathological or physiological processes (Fell et al., 1996; Shen et al., 2003; Micheloyannis et al., 2003) Hence, the a posteriori conclusion that STSA techniques are most suitable for a characterization of neuronal dynamics in general cannot be drawn.

Although our STSA analysis was not primarily designed as a hypothesis test, our results imply that this null hypothesis would have been rejected more often for the EEG recorded in the focal hemisphere than for the non-focal hemisphere. A possible explanation of this finding, which is in close agreement with Casdagli et al. (1997) and Andrzejak et al. (2001a,b), is that the epileptic process induces or enhances nonlinear
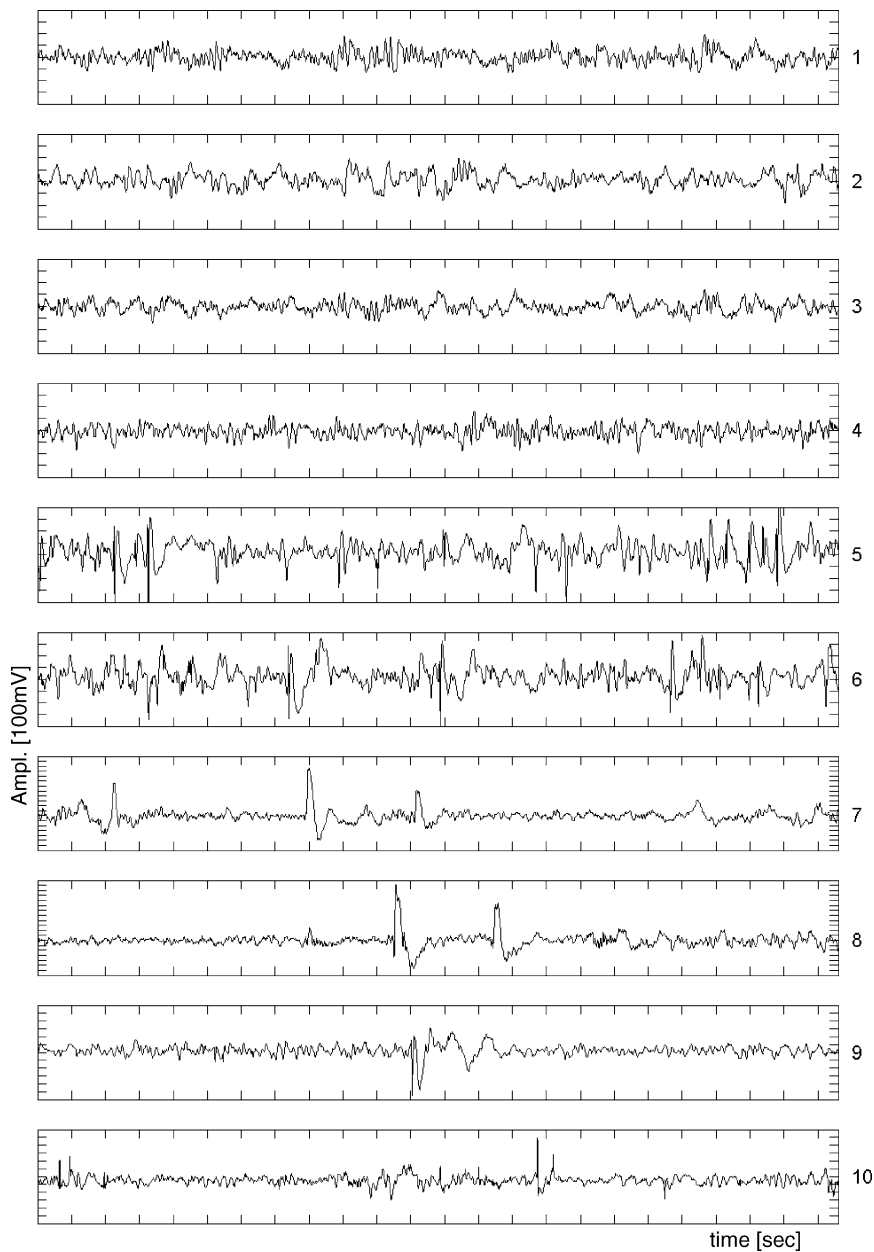
Fig. 4. Exemplary EEG time series. Results for these time series are shown in Fig. 3. Ticks at the abscissa and ordinate are each distant by 1 s and 100 mV, respectively.

deterministic structures in an otherwise linear stochastic appearance of the EEG. There is, however, only little direct evidence for this explanation, and it is important to realize that there are numerous different reasons for a rejection of the surrogates' null hypothesis. In other words, in general the complementary hypothesis is very comprehensive and thus can be quite unspecific: non-linear deterministic dynamics, a non-invertible measurement function, a non-Gaussian random process, non-stationarity of the underlying dynamical system.
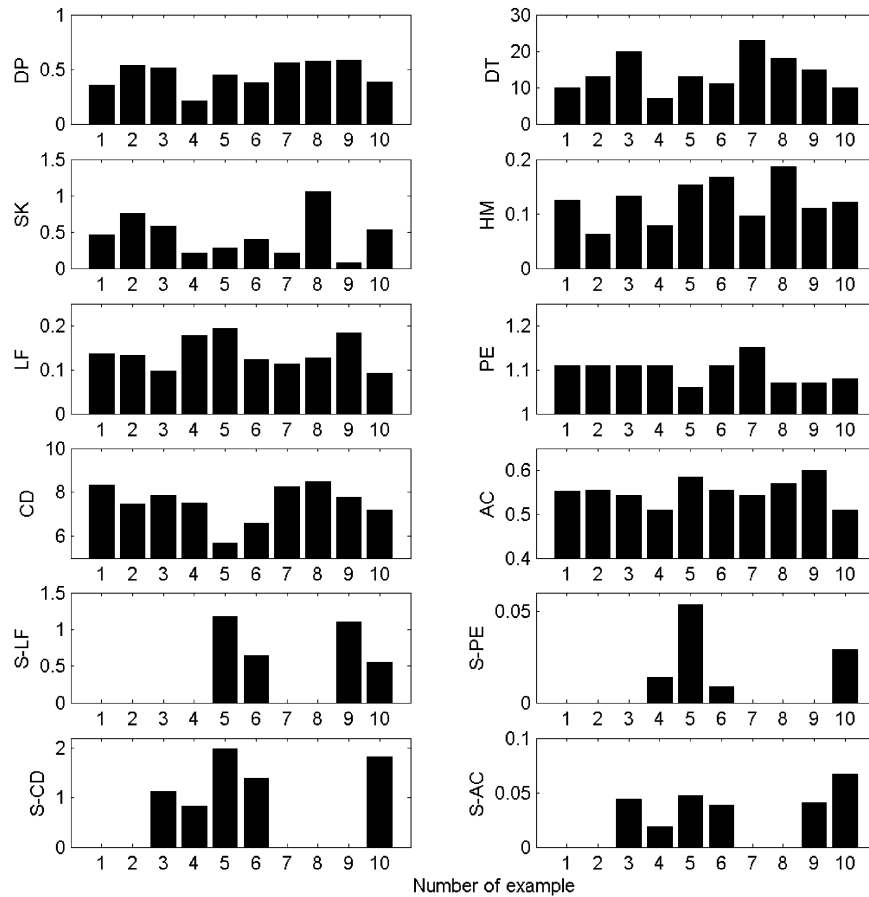
Fig. 5. Results for the exemplary EEG time series shown in Fig. 2. The numbering of the abscissa corresponds to the top-to-bottom order of the examples in Fig. 2.

This list could be continued with many further aspects not explicitly included in the null hypothesis and there is not much reason to assume any of these alternatives as more likely than the others. For a detailed discussion of the caveats related to the application of surrogate techniques, refer to Ref. (Schreiber and Schmitz, 2000; Andrzejak et al., 2003b).

A clinician might take a more pragmatic point of view by asking if a given analysis can render useful information for diagnostic purposes. Indeed the present study demonstrates that in particular STSA techniques can extract valuable information from the EEG of epilepsy patients. With a performance of up to 93% correct lateralizations, these measures can provide valuable additional information during the presurgical evaluation, particularly in cases where findings

obtained by conventional diagnostics are inconsistent. This view is in close agreement with results of Casdagli et al. (1997), who were the first to consider the capability of STSA techniques for epileptic focus localization and who suggested that such techniques 'may prove useful in detecting epileptogenic foci during interictal as well as ictal periods'. In this context it is important to emphasize that our results were obtained solely from the analysis of seizure-free intervals of the patients, i.e. without the necessity of observing actual seizure activity. Although patients with unilateral hippocampal sclerosis nowadays are often operated without prior invasive presurgical evaluation, there are still cases where implantation of intrahippocampal electrodes becomes necessary, e.g. patients with unilateral hippocampal sclerosis and late bitemporal electrographical seizure

onset in noninvasive EEG monitoring. In these cases the proposed techniques could render additional diagnostic information. Furthermore it can be assumed that the proposed techniques could also be applied to invasive recordings obtained from neocortical epilepsies (Andrzejak et al., 1999; Elger et al., 2000; Widman et al., 2000). A particularly well-suited field of application could be focus localization from grid electrodes in nonlesional neocortical epilepsies.

An important issue with regard to the practical feasibility of a certain technique in a clinical setup is the computational expenditure. It needs to be pointed out that the high performance of STSA techniques comes at the price of long computation times. NTSA algorithms are by orders of magnitude more time consuming than LTSA algorithms. Moreover, for STSA techniques the algorithm for the generation of surrogates and the need to run NTSA algorithms repeatedly, namely, for the original and the surrogate time series has to be taken into account. However, thanks to the rapid development of computer technology and the high performance of distributed computing solutions (Müller et al., in press) a real-time calculation of STSA measures for long-term multi-channel EEG recordings becomes more and more feasible in a standard clinical environment.

We conclude that nonlinear methods can be highly relevant and more effective than linear methods for a characterization of neuronal dynamics, provided that they are combined with surrogates. This characterization might on the one hand yield valuable diagnostic information. On the other hand it can advance our understanding of the complicated dynamical system brain.

Acknowledgements

Appendix A

Assuming a dynamical system can be fully described by d variables $y_1(t),\ldots,y_d(t)$, we can achieve a geometrical representation of the dynamics in an abstract d-dimensional state space by constructing a time dependent state vector $v(t) = (y_1(t), \ldots, y_d(t))$. While the system evolves in time, the vector passes through the state space along the so-called trajectory. Each state of the system is represented by a point on this trajectory and vice versa. Basis for time series analysis, however, are scalar valued time series $\{x_n\}$ derived from dynamical systems by means of some measurement function $x_n = g(v(t_n))$ at $n=0,\ldots,N-1$ discrete times. At a given sampling frequency f_s, consecutive measurements are separated by one sampling time: $\tau_s = 1/f_s$.

A.1. Linear time series analysis (LTSA)

The information contained in consecutive amplitude values of a time series can also be encoded by amplitudes and phases of harmonic oscillations with a range of wavelengths or frequencies, respectively (Box and Jenkins, 1976). The discrete Fourier transform, a central concept of LTSA, translates between the two underlying representations of the time domain and the frequency domain. The discrete Fourier transform of $\{x_n\}$ will be denoted as $\{s_k\}$ for $k = -N/2,\ldots,N/2$, with $k = Nf/f_s$ for any given frequency $f \leq f_s/2$. The periodogram is given by the square of the amplitudes of the Fourier transform: $\{p_k\} = \{|s_k^2|\}$. In this paper we do not distinguish between the periodogram and the power spectrum and use the latter term for simplicity. For real valued time series the power spectrum is symmetric with regard to positive and negative values of k, and hence we can simplify formulas in confining them to positive values of k. In that way, the total power of the time series reads $P = \sum_{k=1}^{N/2} p_k$. (For simplification of a number of formulas we assume that the time series' mean values are set to zero prior to analysis.)

A.1.1. Delta power-DP
The delta power quantifies the fraction of power that is contained within the frequency range between 0.5 and 4 Hz, normalized by the total power:

$$DP = \frac{1}{P} \sum_{0.5\,Hz}^{4\,Hz} p_k.$$

Therefore, high values of DP reflect a high fraction of slow activity.

A.1.2. Hjorth mobility-HM

Hjorth defined activity, mobility, and complexity as 'a set of parameters intended as a clinically useful tool for the quantitative description of an EEG' (Hjorth, 1970). All parameters can be formulated and calculated in the time or in the frequency domain, alternatively. The mobility is defined as the variance of the distribution of the local slopes normalized by the variance of the amplitude distribution of the time series. In the frequency domain the mobility is the second statistical moment of the power spectrum normalized by the total power:

$$\mathrm{HM} = \frac{1}{P} \sum_{0.5\,\mathrm{Hz}}^{0.5 f_s} p_k k^2.$$

High values of HM are obtained for spectra with a high fraction of fast activity.

A.1.3. Skewness-SK

Statistical moments describe different properties of the amplitude distribution of a time series (Box and Jenkins, 1976). The second and third moment are given by the variance $\sigma^2 = \frac{1}{N-1}\sum_{i=0}^{N-1} x_i^2$ and by the skewness $\chi = \frac{1}{N}\sum_{i=0}^{N-1}\left(\frac{x_i}{\sigma}\right)^3$, respectively. Note that the variance is proportional to the total power of the time series. The skewness is zero for symmetric amplitude distribution and non-zero values are obtained for asymmetric amplitude distributions. Neglecting the direction of the asymmetry, which could be read from the sign of the skewness, we here define:

$$\mathrm{SK} = |\chi|.$$

High values of SK correspond to highly asymmetric amplitude distributions.

A.1.4. Decay time-DT

The autocorrelation function of a time series (Box and Jenkins, 1976) is defined as $A(\tau) = \frac{1}{(N-1)\sigma^2}\sum_{n=1}^{N-1} x_n x_{n-\tau}$ for $\tau = 1,\ldots,N-1$. Due to the normalization to the variance, $A(0) = 1$ holds by construction. Provided that the time series is non-periodic, the autocorrelation function decays from $A(0)$ with increasing values of the time lag τ, and fluctuates around zero for larger τ-values. The slower $A(\tau)$ decays initially, the stronger are the linear correlations of the time series. Hence, an estimate of linear correlations

can be defined using the decay time:

$$\mathrm{DT} = \{\tau | A(\tau) < A(0)/e\}_{\min}.$$

High values of DT reflect a slowly decaying autocorrelation function.

A.2. Nonlinear time series analysis (NTSA)

While LTSA measures are calculated directly from the time series or the power spectrum a number of NTSA measures were designed to quantify different properties of state space trajectories (Kantz and Schreiber, 1997). Calculation of these NTSA measures therefore requires reconstruction of the state space trajectory from the single valued time series. This can be achieved by means of delay coordinates $z_n = (x_n, x_{n-\tau}, \ldots, x_{n-(m-1)\tau})$ (Takens, 1980). Here τ is the time delay and m is the embedding dimension.

A.2.1. Estimate of an effective correlation dimension-CD

For deterministic dynamics an effective correlation dimension allows to estimate the number of active degrees of freedom (Grassberger and Procaccia, 1983). To this purpose, the correlation sum that counts the number of pairs of points in state space that are closer than a given hypersphere radius ε, is calculated as a function of ε:

$$C(\varepsilon) = \frac{1}{(N-T)(N-T-1)} \sum_{i=0}^{N-1}$$
$$\times \sum_{j=i+T}^{N-1} \Theta(\varepsilon - \|z_i - z_j\|)$$

where $\|\,\|$ indicates the maximum norm and Θ denotes the Heaviside step function ($\Theta(a) = 0$ for $a \leq 0$ and $\Theta(a) = 0$ for $a > 0$). The exclusion of pairs closer in time than the length of the so-called Theiler window T is essential to reduce the unwanted influence of linear correlations on $C(\varepsilon)$ (Theiler, 1986). The correlation dimension is defined as $D_2 = \lim_{N\to\infty}\lim_{\varepsilon\to 0} d(\varepsilon)$ where $d(\varepsilon)$ denotes the local slope $d(\varepsilon) = \frac{\partial \ln C(\varepsilon)}{\partial \ln \varepsilon}$. From the limites it follows that the calculation of the correlation dimension would require an infinite length and an unlimited accuracy of the time series. However, an estimate of an effective correlation dimension can be obtained if

an almost constant value of $d(\varepsilon)$ is found at least for a range of ε values, the so-called quasi-scaling region.

Here we calculated $d(\varepsilon)$ for embedding dimensions $m = 1$ and $m = 25$ using a fixed time delay ($\tau = 1\tau_s$) and Theiler window ($T = 5\tau_s$). The range of ε was chosen to match the resolution of the analog-to-digital converter and was divided into 128 intervals. A quasi-scaling region $[\varepsilon_l, \varepsilon_u]$ is defined by $\varepsilon_u = \max\{\varepsilon | d(\varepsilon)_{|m=1} > 0.975\}$ and $\varepsilon_l = \min\{\varepsilon | d(\varepsilon_u)_{|m=25} - d(\varepsilon)_{|m=25} | \leq 0.05 d(\varepsilon)_{|m=25}\}$. If ε_u and ε_l existed and the number N_r of ε values in $[\varepsilon_l, \varepsilon_u]$ was greater than 4, the estimate $CD = \frac{1}{N}\sum_{\varepsilon=\varepsilon_l}^{\varepsilon_u} d(\varepsilon)_{|m=25}$ was computed. If no quasi-scaling behavior was found for $d(\varepsilon)$ or if $CD \geq 9.5$, an arbitrary but fixed value of $CD = 10$ was set. Low values of CD should be obtained for finite dimensional deterministic dynamics whereas high dimensional stochastic dynamics should result in high values of CD.

A.2.2. Nonlinear prediction error-PE

The unambiguous relation between present and future states that characterizes deterministic dynamics is reflected by the fact that corresponding state space trajectories show no self-intersections. Furthermore, in the case of smooth deterministic dynamics, where similar present states lead to similar evolutions in the near future, nearby trajectory segments are aligned with each other. In contrast, trajectories of stochastic dynamics exhibit self-intersections and nearby segments can enclose arbitrary angles. This distinctive feature of deterministic and stochastic dynamics is used by the nonlinear prediction error (Kantz and Schreiber, 1997; and references therein). After state space reconstruction ($m = 6$, $\tau = 6$), for each reference point z_i the $k = 5$ nearest neighbors $\{z_{j_s}\}_{s=1,\dots,k}$ were determined, where j_s denotes the time index for each respective neighbor. Based on the future evolution of these neighboring points in state space, a prediction for the future evolution of the reference point was performed by calculating $\tilde{z}_{i+H} = \frac{1}{k}\sum_{s=1}^{k} z_{j_s+H}$, where the prediction horizon H was set to 65 sampling times. The difference between the predicted and the actual value $e_{i,\tilde{z}_{i+H}} = |z_{i+H} - \tilde{z}_{i+H}|$ is the local prediction error. The local prediction error for the mean of the time series is $e_{i,\bar{z}} = |z_{i+H} - \bar{z}|$. Here $\bar{z}$ is a vector that carries the mean of the time series in each of its components, i.e. $\bar{z} = \vec{0}$ for a demeaned time series. Finally, the nonlinear

prediction error is defined by

$$PE = \frac{RMS(e_{i,\tilde{z}_{i+H}})}{RMS(e_{i,\bar{z}})}$$

where RMS denotes the root mean square. For the determination of the nearest neighbors a Theiler window ($T = 25\tau_s$) was applied to the reference point and also to the nearest neighbors: First, points were only taken as nearest neighbors if their time index differed by at least T from the time index of the reference point. Second, if remaining points were closer to each other in time than T, only the one nearest to the reference point was included (Farmer and Sidorowich, 1988; Andrzejak et al., 2001b). Low values of PE are obtained for deterministic dynamics whereas high values of PE are attained for stochastic dynamics.

A.2.3. Local flow-LF

For both the correlation sum and the nonlinear prediction error all points on the trajectory are used subsequently as the reference point for all other points. Around this center either a number of points or a radius is fixed to select points to be processed for further statistics. A different approach is used for the calculation of the local flow (Kaplan and Glass, 1992) that aims at discriminating deterministic from stochastic dynamics. For this technique the reconstructed m-dimensional state space is divided into b^m non-overlapping hyper-cubes where b denotes the number of hyper-cubes per state space axis. If the hyper-cube with index j is passed n_j-times by the trajectory, a normalized tangent vector $v_{j,k}$ is generated for each pass ($k = 1,\dots,n_j$) whose direction is determined by connecting the points where the trajectory enters and leaves the hyper-cube. Summing up all vectors of passes through hyper-cube j, the resultant vector V_j, normalized by the number of passes n_j, is $V_j = \frac{1}{n_j}\sum_{k=1}^{n_j} v_{j,k}$. The expected absolute value for a vector addition of n vectors of unit length yielded by a random walk in m dimensions is: $R \propto \frac{1}{\sqrt{n}}$. Accordingly, the following average is constructed over all occupied hyper-cubes: $\Lambda = \sum_j \frac{V_j^2 - R^2}{1 - R^2}$.

Using an embedding dimension of $m = 6$, the number of hyper-cubes per state space axis was determined empirically from the range and the variance of the time series according to $b = 0.875\frac{\max\{x_n\} - \min\{x_n\}}{\sigma^2}$, resulting in values of b from 6 to 20. Rather than using a fixed

time delay τ the local flow was calculated as

$$LF = \frac{1}{16}\sum_{\tau=5}^{20} \Lambda(\tau).$$

High values of LF reflect deterministic dynamics whereas low values of LF are obtained for stochastic dynamics.

A.2.4. Algorithmic complexity-AC

Rather than using delay coordinates to reconstruct the state space the time series was transformed into a symbol sequence for the calculation of the algorithmic complexity. For this purpose the range of amplitude values was partitioned, and a different symbol S is assigned to each interval. Then each value of the time series is replaced by the symbol of its interval. The thresholds of the partition were chosen separately for each time series to yield a homogenous distribution of symbols. To achieve a good statistics as well as a good representation of the time series, the number of different symbols was set to $A = 16$.

The resulting symbol sequence $\{S_i\}$ with $i = 1,\ldots,N$ was then investigated for its complexity by estimating the size $c(\{S_i\})$ of its vocabulary. This size was defined as the number of different words in a Lempel–Ziv parsing (Lempel and Ziv, 1976) of the symbol sequence. In this algorithm the symbol sequence is scanned from the beginning to its end, and $c(\{S_i\})$ is increased by 1 unit as soon as a new subsequence of consecutive symbols is encountered in the scanning process (Kasper and Schuster, 1987) and the following symbol is regarded as the beginning of the next symbol sequence. This value is normalized by the expected asymptotic value for a random sequence of symbols of length N to yield the algorithmic complexity:

$$AC = \frac{\log_A N}{N} c\{S_i\}$$

Low values of AC are obtained for deterministic dynamics whereas high values of AC reflect stochastic dynamics.

A.3. Surrogate time series analysis (STSA)

The concept of surrogates was developed to test a specified null hypothesis about the dynamics underlying a time series under investigation. In our study we applied an iterative algorithm proposed by Schreiber and Schmitz (Schreiber and Schmitz, 1996). Starting from a random permutation of the original samples of the time series, these surrogates are constructed by an iterative algorithm that alternately adjusts the periodogram and the amplitude distribution to the original values, resulting in a deviation of the respective other quantity. After a sufficient number of iterations (typically 20–200) deviations of both quantities from values of the original time series are reduced to negligibly small values. Hence, the surrogate time series will have practically the same power spectrum and amplitude distribution as the original time series. In consequence, any LTSA measures would have practically the same result for the original time series and its surrogates. In combination with NTSA measures, which are sensitive to properties beyond the power spectrum and amplitude distribution, these surrogates allow testing the null hypothesis that the original time series was measured from a stationary Gaussian linear stochastic dynamics by means of a static and invertible measurement function. If the NTSA measure for the original deviates significantly from the distribution of the values obtained for the surrogates, this null hypothesis can be rejected. For the interpretation of such a rejection, which has do be done with care, refer to the discussion in the body text and to Refs. (Schreiber and Schmitz, 2000; Andrzejak et al., 2003b). In the present study we use the surrogates not primarily as a means to test against a null hypothesis, but rather as an offset correction by defining the STSA measures as

$$S\text{-}LF = \begin{cases} LF_{EEG} - \overline{LF_{SUR}} & \text{if } LF_{EEG} - \overline{LF_{SUR}} > 0 \\ 0 & \text{else} \end{cases}$$

$$S\text{-}CD = \begin{cases} \overline{CD_{SUR}} - CD_{EEG} & \text{if } \overline{CD_{SUR}} - CD_{EEG} > 0 \\ 0 & \text{else} \end{cases}$$

$$S\text{-}AC = \begin{cases} \overline{AC_{SUR}} - AC_{EEG} & \text{if } \overline{AC_{SUR}} - AC_{EEG} > 0 \\ 0 & \text{else} \end{cases}$$

$$S\text{-}PE = \begin{cases} \overline{PE_{SUR}} - PE_{EEG} & \text{if } \overline{PE_{SUR}} - PE_{EEG} > 0 \\ 0 & \text{else} \end{cases}$$

Here the over-bar denotes mean values obtained for a set of nine surrogates. For a stationary linear stochas-

tic dynamics there should be no difference between NTSA values for the original time series and the surrogates. Accordingly, one should obtain S-LF ≈ 0, S-CD ≈ 0, S-AC ≈ 0, and S-PE ≈ 0. For a nonlinear deterministic dynamics, values of LF should be higher for the surrogates, and values of CD, AC, and PE should be lower for the surrogates. (Recall that a linear stochastic dynamics results in low values of LF and in high values of CD, AC, and PE.) For the sake of intuitiveness and homogeneity we therefore introduced the pre-factor of (-1) in the definitions of S-CD, S-AC, and S-PE. Defined in this way, all four STSA measures attain *positive* values for nonlinear deterministic dynamics and values close to zero for linear stochastic dynamics.

Note that the surrogate null hypothesis test is two-sided. The value of an NTSA measure such as LF obtained for the original time series can be higher than the mean value obtained for the surrogates, resulting in non-zero values of the corresponding STSA measure S-LF, but it can also be lower. In our experience, this latter event occurs particularly often for distinctively nonstationary time series (cf. Andrzejak et al., 2001b). In order to reduce the influence of nonstationarity on our results, we therefore deliberately set the STSA measures to zero in this case (corresponding to the 'else' case in the above definitions. For the other STSA measures analogous relations hold.

References

Andrzejak, R.G., Widman, G., Lehnertz, K., David, P., Elger, C.E., 1999. Nonlinear determinism in intracranial EEG recordings allows focus localization in neocortical lesional epilepsy. Epilepsia 40 (Suppl. 7), 171–172.

Andrzejak, R.G., Widman, G., Lehnertz, K., Rieke, C., David, P., Elger, C.E., 2001a. The epileptic process as nonlinear deterministic dynamics in a stochastic environment—an evaluation of mesial temporal lobe epilepsy. Epilepsy Res. 44, 129–140.

Andrzejak, R.G., Lehnertz, K., Rieke, C., David, P., Elger, C.E., 2001b. Indications of nonlinear deterministic and finite-dimensional structures in time series of brain electrical activity: dependence on recording region and brain state. Phys. Rev. E 64, 061907.

Andrzejak, R.G., Mormann, F., Kreuz, T., Rieke, C., Kraskov, A., Elger, C.E., Lehnertz, K., 2003a. Testing the null hypothesis of the non-existence of the pre-seizure state. Phys. Rev. E 67, 010901.

Andrzejak, R.G., Kraskov, A., Stögbauer, H., Mormann, F., Kreuz, T., 2003b. Bivariate surrogate techniques: necessity, strengths, and caveats. Phys. Rev. E 68, 066202.

Babloyantz, A., Destexhe, A., 1986. Low-dimensional chaos in an instance of epilepsy. Proc. Natl. Acad. Sci. U.S.A. 83, 3513–3517.

Box, G.E.P., Jenkins, G.M., 1976. Time Series Analysis. Holden-Day, San Fransisco, USA.

Casdagli, M.C., Iasemides, L.D., Savit, R.S., Gilmore, R.L., Roper, S.N., Sackellares, J.C., 1997. Non-linearity in invasive EEG recordings from patients with temporal lobe epilepsy. Electroencephalogr. Clin. Neurophysiol. 102, 98–105.

Drake, M.E., Padamadan, H., Newell, S.A., 1998. Interictal quantitative EEG in epilepsy. Seizure 7, 39–42.

Ehlers, C.L., Havstad, J., Prichard, D., Theiler, J., 1998. Low doses of ethanol reduce evidence for nonlinear structure in brain activity. J. Neurosci. 18, 7468–7474.

Elger, C.E., Widman, G., Andrzejak, R., Arnhold, J., David, P., Lehnertz, K., 2000. Value of nonlinear time series analysis of the EEG in neocortical epilepsies. Adv. Neurol. 84, 317–330.

Farmer, J.D., Sidorowich, J.J., 1988. Exploiting chaos to predict the future and reduce noise. In: Lee, YC. (Ed.), Evolution, Learning, and Cognition. World Scientific, Singapore, pp. 277–330.

Fell, J., Röschke, J., Mann, K., Schaffner, C., 1996. Discrimination of sleep stages: a comparison between spectral and nonlinear EEG measures. Electroencephalogr. Clin. Neurophysiol. 98, 401–410.

Frank, G.W., Lookman, T., Nerenberg, M.A.H., Essex, C., Lemieux, J., Blume, W., 1990. Chaotic time series analyses of epileptic seizures. Phys. D 46, 427–438.

Gambardella, A., Gotman, J., Cendes, F., Andermann, F., 1995. Focal intermittent delta activity in patients with mesiotemporal atrophy: a reliable marker of the epileptogenic focus. Epilepsia 36, 122–129.

Grassberger, P., Procaccia, I., 1983. On the strangeness of strange attractors. Phys. Rev. Lett. 50, 346–349.

Hjorth, B., 1970. EEG analysis based on time domain properties. Electroencephalogr. Clin. Neurophysiol. 29, 306–310.

Kantz, H., Schreiber, T., 1997. Nonlinear Time Series Analysis. Cambridge University Press, Cambridge, UK.

Kaplan, D.T., Glass, L., 1992. Direct test for determinism. Phys. Rev. Lett. 68, 427–430.

Kasper, F., Schuster, H.G., 1987. Easily calculable measure for the complexity of spatiotemporal patterns. Phys. Rev. A 36, 842–848.

Kugiumtzis, D., Larson, P.G., 2000. Linear and nonlinear analysis of the EEG for the prediction of epileptic seizures. In: Lehnertz, K., Arnhold, J., Grassberger, P., Elger, C.E. (Eds.), Chaos in Brain? World Scientific, Singapore, pp. 329–332.

Lehnertz, K., Elger, C.E., 1995. Spatio-temporal dynamics of the primary epileptogenic area in temporal lobe epilepsy characterized by neuronal complexity loss. Electroencephalogr. Clin. Neurophysiol. 95, 108–117.

Lempel, A., Ziv, J., 1976. On the complexity of finite sequences. IEEE Trans. Inform. Theory 22, 75–81.

Li, D.Z., Zhou, W.P., Drury, I., Savit, R., 2003. Linear and nonlinear measures and seizure anticipation in temporal lobe epilepsy. J. Comp. Neurosci. 15, 335–345.

Marciani, M.G., Stefanini, N., Stefanini, F., Maschio, M.C.E., Gigli, G.L., Bernardi, G., Caltagirone, C., 1992. Lateralization of the epileptogenic focus by computerized EEG study and neuropsychological evaluation. Int. J. Neurosci. 66, 53–60.

McSharry, P., Smith, L.A., Tarassenko, L., 2003. Prediction of epileptic seizures: are nonlinear methods relevant? Nat. Med. 9, 241–242.

Micheloyannis, S., Vourkas, M., Bizas, M., Simos, P., Stam, C.J., 2003. Changes in linear and nonlinear EEG measures as a function of task complexity: evidence for local and distant signal synchronization. Usefulness of non-linear EEG analysis. Brain Topogr. 15, 239–247.

Mormann, F., Andrzejak, R.G., Kreuz, T., Rieke, C., David, P., Lehnertz, K., Elger, C.E., 2003. Automated detection of a preseizure state based on a decrease in synchronization in intracranial electroencephalogram recordings from epilepsy patients. Phys. Rev. E 67, 021912.

Mormann, F., Kreuz, T., Rieke, C., Andrzejak, R.G., Kraskov, A., David, P., Elger, C.E., Lehnertz, K., 2005. On the predictability of epileptic seizures. Clin. Neurophysiol. 116, 569–587.

Mormann, F., Lehnertz, K., David, P., Elger, C.E., 2000. Mean phase coherence as a measure for phase synchronization and its application to the EEG of epilepsy patients. Physica D 144, 358–369.

Müller, A., Osterhage, H., Sowa, R., Andrzejak, R.G., Mormann, F., Lehnertz, K., 2006. A distributed computing system for multivariate time series analyses of multichannel neurophysiological data. J. Neurosci. Meth. 152, 190–201.

Niedermeyer, E., Lopes da Silva, F.H., 1999. Electroencephalography. Williams and Wilkins, Baltimore, USA.

Nuwer, M.R., 1988. Frequency analysis and topographic mapping of EEG and evoked potentials in epilepsy. Electroencephalogr. Clin. Neurophysiol. 69, 118–126.

Osborne, A.R., Provenzale, A., 1989. A finite correlation dimension for stochastic systems with power-law spectra. Phys. D 35, 357–381.

Paluš, M., Komárek, V., Hrnčíř, Z., Procházka, T., 1999. Is nonlinearity relevant for detecting changes in EEG? Theory Biosci. 118, 179–188.

Panet-Raymond, D., Gotman, J., 1990. Asymmetry in delta activity in patients with focal epilepsy. Electroencephalogr. Clin. Neurophysiol. 75, 474–481.

Pijn, J.P., van Neerven, J., Noest, A., Lopes da Silva, F., 1991. Chaos or noise in EEG signals; dependence on state and brain site. Electroencephalogr. Clin. Neurophysiol. 79, 371–381.

Pijn, J.P., Velis, D.N., van der Heyden, M.J., DeGoede, J., van Veelen, C.W., Lopes da Silva, F.H., 1997. Nonlinear dynamics of epileptic seizures on basis of intracranial EEG recordings. Brain Topogr. 9, 249–270.

Schreiber, T., Schmitz, A., 1996. Improved surrogate data for nonlinearity tests. Phys. Rev. Lett. 77, 635–638.

Schreiber, T., Schmitz, A., 2000. Surrogate time series. Phys. D 142, 346–382.

Shen, Y., Olbrich, E., Achermann, P., Meier, P.F., 2003. Dimensional complexity and spectral properties of the human sleep EEG. Clin. Neurophysiol. 114, 199–209.

Takens, F., 1980. Detecting strange attractors in turbulence. In: Rand, D.A., Young, LS. (Eds.), Dynamical Systems and Turbulence. Lecture Notes in Mathematics, vol. 898. Springer-Verlag, Berlin, Germany, pp. 366–381.

Theiler, J., 1986. Spurious dimensions from correlation algorithms applied to limited time-series data. Phys. Rev. A 34, 2427–2432.

Tuunainen, A., Nousiainen, U., Pilke, A., Mervaala, E., Partanen, J., Riekkinen, P., 1995. Spectral EEG during short-term discontinuation of antiepileptic medication in partial epilepsy. Epilepsia 36, 817–823.

Van Roost, D., Solymosi, L., Schramm, J., Van Oosterwyck, B., Elger, C.E., 1998. Depth electrode implantation in the length axis of the hippocampus for the presurgical evaluation of medial temporal lobe epilepsy: a computed tomography-based stereotactic insertion technique and its accuracy. Neurosurgery 43, 819–827.

Wang, J., Wieser, H.G., 1994. Regional "rigidity" of background EEG activity in the epileptogenic zone. Epilepsia 35, 495–504.

Weber, B., Lehnertz, K., Elger, C.E., Wieser, H.G., 1998. Neuronal complexity loss in interictal EEG recorded with foramen ovale electrodes predicts side of primary epileptogenic area in temporal lobe epilepsy: a replication study. Epilepsia 39, 922–927.

Widman, G., Lehnertz, K., Urbach, H., Elger, C.E., 2000. Spatial distribution of neuronal complexity loss in neocortical epilepsies. Epilepsia 41, 811–817.

Winterhalder, M., Maiwald, T., Voss, H.U., Aschenbrenner-Scheibe, R., Timmer, J., Schulze-Bonhage, A., 2003. The seizure prediction characteristic: a general framework to assess and compare seizure prediction methods. Epilepsy Behav. 4, 318–325.